nature chemical biology

ARTICLE

PUBLISHED ONLINE: 25 MARCH 2012 | DOI: 10.1038/NCHEMBIO.922

Rapid and orthogonal logic gating with a gibberellin-induced dimerization system

Takafumi Miyamoto[1,5], Robert DeRose[1,5], Allison Suarez[1], Tasuku Ueno[1], Melinda Chen[1], Tai-ping Sun[2], Michael J Wolfgang[3], Chandrani Mukherjee[4], David J Meyers[4] & Takanari Inoue[1]*

Using a newly synthesized gibberellin analog containing an acetoxymethyl group (GA_3-AM) and its binding proteins, we developed an efficient chemically inducible dimerization (CID) system that is completely orthogonal to existing rapamycin-mediated protein dimerization. Combining the two systems should allow applications that have been difficult or impossible with only one CID system. By using both chemical inputs (rapamycin and GA_3-AM), we designed and synthesized Boolean logic gates in living mammalian cells. These gates produced output signals such as fluorescence and membrane ruffling on a timescale of seconds, substantially faster than earlier intracellular logic gates. The use of two orthogonal dimerization systems in the same cell also allows for finer modulation of protein perturbations than is possible with a single dimerizer.

We aimed to create fast-processing logic gates based on CID systems. CID is a tool for inducible, rapid and specific manipulation of various signaling molecules in living cells[1,2]. Rapamycin, the most commonly used chemical dimerizer, induces interaction between FK506-binding protein (FKBP) and FKBP-rapamycin-binding protein (FRB)[3,4]; this system originates from use of FK1012 as a synthetic dimerizer in 1993 (ref. 5). This principle has been used to manipulate various aspects of cell signaling, thereby resolving biological questions that were otherwise challenging[6–9]. Recent efforts have attempted to expand the palette of CID systems[10–13], aiming to control multiple signaling molecules at the same or different times and locations. However, so far, no two systems have been simultaneously orthogonal to each other and working on a rapid timescale in the context of a living cell. These conditions are required for fast-processing *in vivo* logic gates. Biomolecular logic gates in a cell-free system have been constructed using nucleotides[14–16] and protein enzymes[17]. Some of them are networked to form large-scale circuits for DNA computing[18]. Several logic gates have also been constructed in living cells, generally based on protein translation as output[19,20] and often using gene circuits[20–23]. The CID system has also been used to create logic gates[24]. Although processing speed is a critical component of computational entities, the timescales of these logic gates in living cells are relatively slow, on the order of tens of minutes to hours. In particular, the slow response time of CID logic gates is at least partly attributed to a time-consuming transcriptional process and slow dimerization (except in the case of rapamycin-mediated dimerization).

In this study, we developed a new CID system using a plant hormone, gibberellin; this system is completely orthogonal to the rapamycin system and works on a timescale of seconds. Recent advances in plant biology have uncovered a molecular mechanism of action by plant hormones[25]. Like other hormones, gibberellins regulate various aspects of plant growth and development. At a molecular level, gibberellin binds its receptor, GIBBERELLIN INSENSITIVE DWARF1 (GID1)[26], and induces a conformational change. This new conformation attracts another protein called GIBBERELLIN INSENSITIVE (GAI)[27] (**Fig. 1a**). These binding events require a very selective gibberellin such as GA_3 (**1**; ref. 28), one of the >100 gibberellin metabolites. We developed and optimized a series of GID1 and GAI fusion proteins that can form a CID system activated by GA_3-AM (**2**), which readily enters mammalian cells and is cleaved by esterases to release active GA_3. We then showed that this gibberellin-mediated CID system is fully orthogonal to rapamycin CID and can be used to induce protein translocation and to move active protein to specific subcellular locations on a timescale of seconds to minutes. Finally, by combining gibberellin- and rapamycin-based CID, we generated intracellular logic gates using two distinct chemical inputs.

RESULTS

Optimizing uptake of gibberellin-based dimerizer

To assess whether GA_3 induces binding of GID1 and GAI in mammalian cells (**Fig. 1a**), we first established a fluorescence resonance energy transfer (FRET) assay by modifying a system reported earlier[28]. We constructed a series of fusion proteins consisting of enhanced fluorescent proteins (cyan fluorescent protein (CFP) or yellow fluorescent protein (YFP)) and *Arabidopsis thaliana* GAI or GID1. First, we expressed CFP-GAI and YFP-GID1 in HeLa epithelial cells to visualize GAI-GID1 interactions upon addition of GA_3 by monitoring FRET between these fusion proteins. We observed a marginal FRET increase over 10 min (**Supplementary Results**, **Supplementary Fig. 1**). We attributed this to inefficient membrane permeability of GA_3, probably owing to a carboxylic acid group that is negatively charged at physiological pH. To improve membrane permeability of GA_3, we esterified the carboxylic acid of GA_3. More specifically, we used an acetoxymethyl (AM) group[29] such that the negative charge of GA_3 was masked until ambient esterases inside cells cleaved the AM ester group to produce a bioactive GA_3 (**Fig. 1a**). We named the esterified compound GA_3-AM (see complete synthetic schemes in **Supplementary Methods**). We then repeated the FRET assay with GA_3-AM instead of GA_3. GA_3-AM induced a robust increase in the FRET signal on a timescale of 60 s (**Supplementary Fig. 1**), indicating that GA_3-AM went into cells, was converted into GA_3 and induced dimerization between CFP-GAI and YFP-GID1. Other combinations of GAI and GID1 with a

[1]Department of Cell Biology, Center for Cell Dynamics, School of Medicine, Johns Hopkins University, Baltimore, Maryland, USA. [2]Department of Biology, Duke University, Durham, North Carolina, USA. [3]Department of Biological Chemistry, School of Medicine, Johns Hopkins University, Baltimore, Maryland, USA. [4]Department of Pharmacology and Molecular Sciences, Synthetic Core Facility, School of Medicine, Johns Hopkins University, Baltimore, Maryland, USA. [5]These authors contributed equally to this work. *e-mail: jctinoue@jhmi.edu

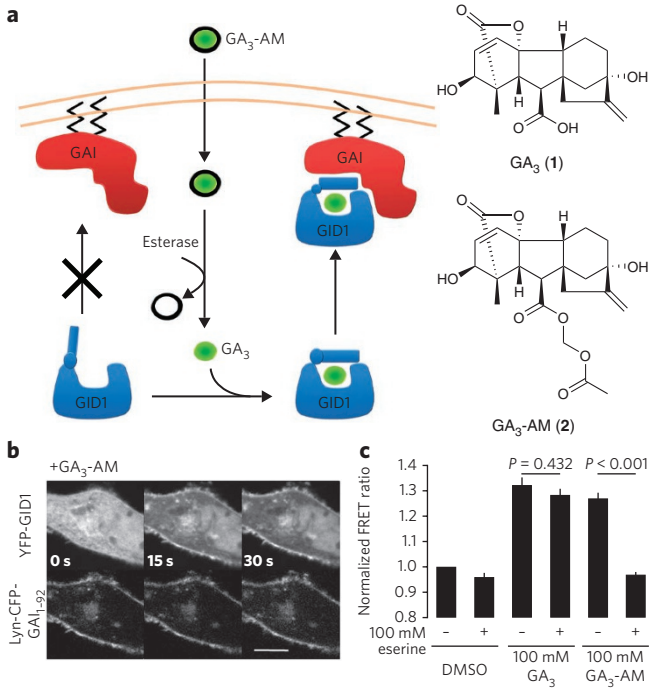

Figure 1 | The gibberellin-inducible CID system functions on a timescale of seconds. (**a**) General scheme of gibberellin-induced CID used in this study. GA_3-AM (**2**; green ball covered with black line) can cross the plasma membrane of target cells, whereupon cytosolic esterase cleaves the AM group to release free GA_3 (**1**; green ball). GA_3 then binds GID1 (blue), which induces formation of a complex between GID1 and GAI (red). (**b**) Time series of confocal fluorescence images of HeLa cells co-transfected with Lyn-CFP-$GAI_{1–92}$ and YFP-GID1. Cells were treated with GA_3-AM (100 μM). Top, YFP fluorescence signal; bottom, CFP fluorescence in same cell. Scale bar, 10 μm. (**c**) Esterase activity is required for GA_3-AM dimerizing ability. Lysate was made of COS-7 cells co-transfected with CFP-$GAI_{1–92}$ and YFP-GID1; eserine (100 μM) was added and FRET was measured 0 and 2 min after addition of DMSO, GA_3 or GA_3-AM. Graph represents mean and s.e.m. of three independent experiments. Statistical analysis was done with unpaired two-tailed Student's *t*-test assuming two populations have same variances.

different configuration (CFP-GAI plus YFP-GID1 or GAI-CFP plus YFP-GID1) also showed a comparable FRET increase. This binding may be more efficient because GA_3 has no known competing binding proteins in mammalian cells.

Optimization of dimerizing proteins

We then determined the minimal domains of GAI and GID1. For a dimerization unit, protein components should be small and devoid of any regulatory domain that may affect cell signaling in an unintended manner. Auxin-induced dimerization of two plant proteins can trigger downstream effects (that is, protein degradation) in mammalian cells, as one of these plant proteins can signal to downstream machinery through a mammalian homolog[30]. Thus, we tested a series of truncated GAIs to identify a minimal GAI domain for GA_3-induced dimerization. Two N-terminal domains (DELLA and TVHYNP) of GAI were sufficient to interact with GID1 in yeast two-hybrid assays[31], whereas a C-terminal GRAS domain interacts with GID1 once the DELLA domain binds GID1 (ref. 32). The GRAS domain also interacts with other proteins including SLY1 and GID2, which in turn targets GAI for degradation via ubiquitin-mediated proteolysis[27]. We therefore constructed three truncated mutants (**Supplementary Fig. 2a**). The first truncated mutant contains the DELLA and VHYNP domains ($GAI_{1–92}$), and the second and third mutants contain additional polyserine and polythreonine domains ($GAI_{1–151}$ and $GAI_{1–172}$). In the FRET assay, all these truncated GAIs bound GID1 upon GA_3-AM addition with similar efficiencies (0.0072 s^{-1}, 0.0095 s^{-1} and 0.0106 s^{-1}, respectively), demonstrating that N-terminal DELLA and TVHYNP are sufficient for dimerization in mammalian cells (**Supplementary Fig. 2b**). The dynamic range of FRET increase for truncated and full-length GAI was correlated with their expression (**Supplementary Fig. 3**).

Gibberellin CID induces protein translocation

Next we assessed how well this new dimerization system controlled protein localization. To recruit proteins from the cytoplasm to the plasma membrane, we modified $GAI_{1–92}$ with 11 amino acid residues of Lyn kinase to target the protein to the plasma membrane[33]; GID1 remained in the cytoplasm without further engineering (**Fig. 1a**). Confocal fluorescence imaging showed that GID1 rapidly changed its localization upon addition of GA_3-AM from the cytoplasm to the plasma membrane in HeLa cells (**Fig. 1b**) and in HEK293T, NIH3T3 and MCF10A cells (**Supplementary Fig. 4**). We determined an apparent rate constant of 0.013 s^{-1} through quantitative analysis of fluorescence intensity of cytoplasmic YFP-GID1 (**Supplementary Fig. 5a**). By varying the concentration of GA_3-AM, we obtained dose-dependent kinetic values, yielding an half-maximum effective concentration (EC_{50}) of 310 nM (**Supplementary Fig. 5b**). We also tested $GAI_{1–151}$, $GAI_{1–172}$ and full-length GAI; all showed membrane translocation of GID1. However, the apparent rate constant of full-length GAI was slower than that of the other GAI truncation mutants (**Supplementary Fig. 5c**), probably owing to low protein expression. In contrast to GAI, GID1 distributes amino acids responsible for dimerization throughout the protein[34,35], making minimization challenging. On the basis of the FRET and translocation assays, we concluded that $GAI_{1–92}$ and full-length GID1 are the best pair for induction of dimerization by gibberellin.

Esterases are required for GA_3-AM–induced dimerization

As our gibberellin-based chemical dimerizer depends on cellular esterases, questions arise regarding the expression of these esterases, their abundance across cells in the population and their enzymatic efficiency. To evaluate these features, we measured the fluorescence intensity of calcein-AM, which fluoresces upon cleavage of AM esters. These esterases are very efficient and are expressed ubiquitously (**Supplementary Fig. 6**). Consistent with this observation, AM-esterified molecular probes are functional in a variety of cell types[36]. To address whether GA_3-AM directly binds to GID1, unlike our initial prediction, we used two approaches: FRET binding assays in cells using a newly synthesized nonhydrolyzable GA_3 analog (GA_3 hydroxamate, or GA_3-H (**3**); see **Supplementary Methods** for synthetic scheme) and *in vitro* FRET binding assays using cell extracts containing GAI and GID1. In the first approach, we observed that GA_3-H induced FRET between GID1 and GAI (**Supplementary Fig. 7a**), but the kinetics of GA_3-H was much slower than that of GA_3 (**Supplementary Fig. 1**). GA_3-H was roughly ten-fold slower than GA_3-AM in the plasma membrane translocation assay, with an apparent rate constant of 0.00103 s^{-1} at 1 mM (**Supplementary Figs. 5b** and **7b**). These results suggest that the carboxylic acid of GA_3 is critical for the binding of GID1. In the second approach, we prepared cell extracts containing YFP-GID1 and CFP-$GAI_{1–92}$ for an *in vitro* FRET assay. We monitored FRET between the two proteins in real time before and after adding DMSO, GA_3 or GA_3-AM to the extract with or without an esterase inhibitor (eserine, 100 μM). Both GA_3 and GA_3-AM induced a FRET increase without eserine (**Fig. 1c**). However, eserine addition inhibited the FRET increase induced by GA_3-AM but not by GA_3 ($P = 0.0003$ versus $P = 0.432$, respectively, **Fig. 1c**). The inhibitory effect of eserine on the GA_3-AM-induced FRET increase depended on eserine concentration

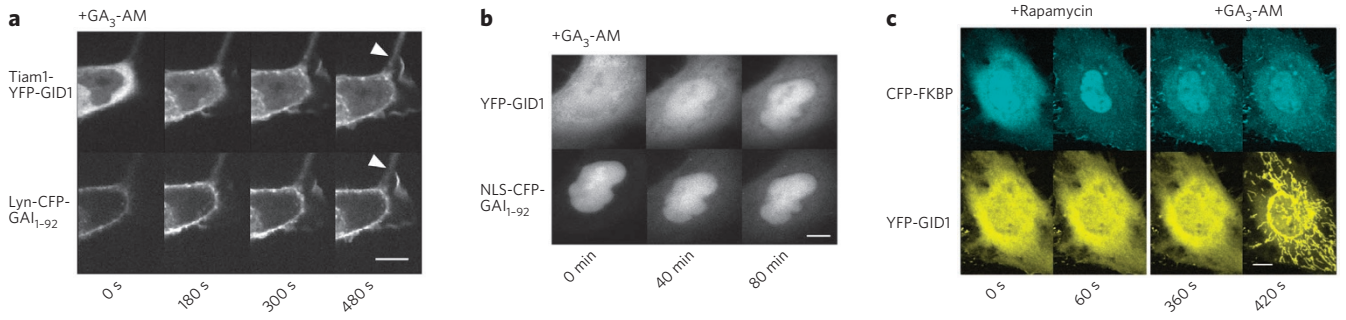

Figure 2 | Gibberellin-based CID can induce localized protein activity and is orthogonal to rapamycin CID. (**a**) Time series of confocal fluorescence images of COS-7 cells transfected with Lyn-CFP-$GAI_{1–92}$ and Tiam1-YFP-GID1 before and after addition of GA_3-AM (100 μM). Arrowheads, ruffles. Same cell is in top (imaged in YFP channel) and bottom (CFP channel) rows. (**b**) Gibberellin CID can be used to translocate proteins to the nucleus. COS-7 cells co-transfected with YFP-GID1 and NLS-CFP-$GAI_{1–92}$ were treated with GA_3-AM (10 μM) and imaged. Representative cell is shown in both CFP and YFP channels. (**c**) Confocal fluorescence images of COS-7 cells transfected with CFP-FKBP and YFP-GID1 together with Lyn-mCherry-FRB and Tom20-mCherry-$GAI_{1–92}$. Images were taken before and after sequential addition of rapamycin and GA_3-AM. Scale bars, 10 μm.

(**Supplementary Fig. 8**). Collectively, these results support the notion that GA_3, but not GA_3-AM itself, induces dimerization of GID1 and GAI in cells.

Gibberellin CID induces localized protein activity

Inducible protein translocation has been used to manipulate activity and concentration of biomolecules[1]. To test whether gibberellin-induced protein translocation can be translated into changes in protein activity, we generated Tiam1-YFP-GID1. Tiam1 is a guanine nucleotide exchanger factor that activates Rac when recruited to the plasma membrane[24]. When the Tiam1-YFP-GID1 construct was expressed in cells with Lyn-CFP-$GAI_{1–92}$, the cells showed robust membrane ruffles after GA_3-AM addition (**Fig. 2a**), indicating that Rac was inducibly activated.

Rapamycin CID has also been used to control transcriptional activity by translocating a transcriptional factor into the nucleus in a rapamycin-dependent manner. To determine whether gibberellin CID could be used in the same context, we constructed a nuclear-localizing GAI (NLS-CFP-$GAI_{1–92}$), which successfully recruited YFP-GID1 from the cytoplasm to the nucleus after addition of GA_3-AM (**Fig. 2b** and **Supplementary Fig. 9**), suggesting its potential use in controlling transcriptional activity. YFP-GID1 was present at a low concentration in the nucleus even before addition of GA_3-AM; its abundance may be increased by adding a nuclear export signal sequence to the YFP-GID1 construct. Another application for a nuclear translocation system is manipulating signals inside the nucleus on a rapid timescale. To this end, we fused a YFP-GID1 to a phosphatase of phosphatidylinositol 4,5-bisphosphate (Inp54p-YFP-GID1). When expressed in cells, the protein was mostly found in the cytoplasm with very little expression in the nucleus. Subsequent GA_3-AM addition induced efficient translocation into the nucleus (**Supplementary Fig. 10**).

Gibberellin and rapamycin CID systems are orthogonal

Rapamycin-induced dimerization and GA_3-induced dimerization should be orthogonal to each other, as they are derived from completely different kingdoms (that is, plant versus animal) and GA_3 and rapamycin share no structural resemblance. To explore this, we carried out a simultaneous translocation assay in which both dimerization systems were introduced in the same cells. Here we intended to recruit CFP-FKBP to the plasma membrane and YFP-GID1 to the mitochondria. More specifically, mCherry-FRB was anchored to the

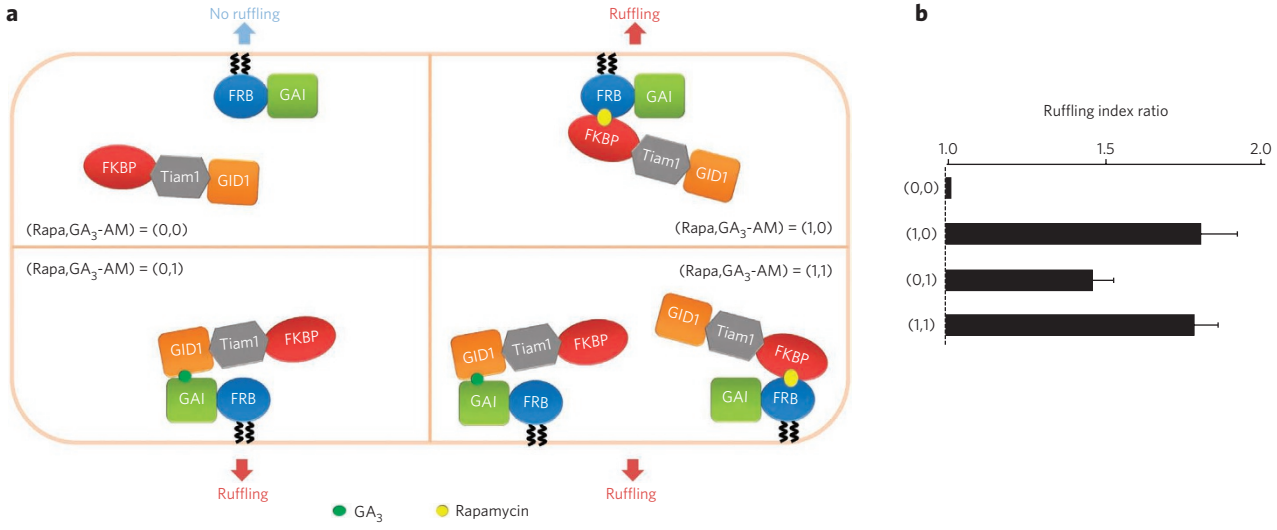

Figure 3 | A fast-processing OR logic gate in living cells using two CID systems. (**a**) Schematic diagram of OR gate using membrane ruffling as output signal; fluorescent reporter molecules are omitted for clarity. Membrane ruffling was measured for COS-7 cells co-transfected with Lyn-CFP-FRB-$GAI_{1–92}$ and FKBP-YFP-Tiam1-GID1 that were subject to treatment with DMSO (representing 0,0 input), rapamycin (Rapa) alone (1,0), GA_3-AM alone (0,1) or rapamycin and GA_3-AM together (1,1). (**b**) Data from OR gate in **a**. Results are mean and s.e.m. ($n \geq 20$, from three independent experiments).

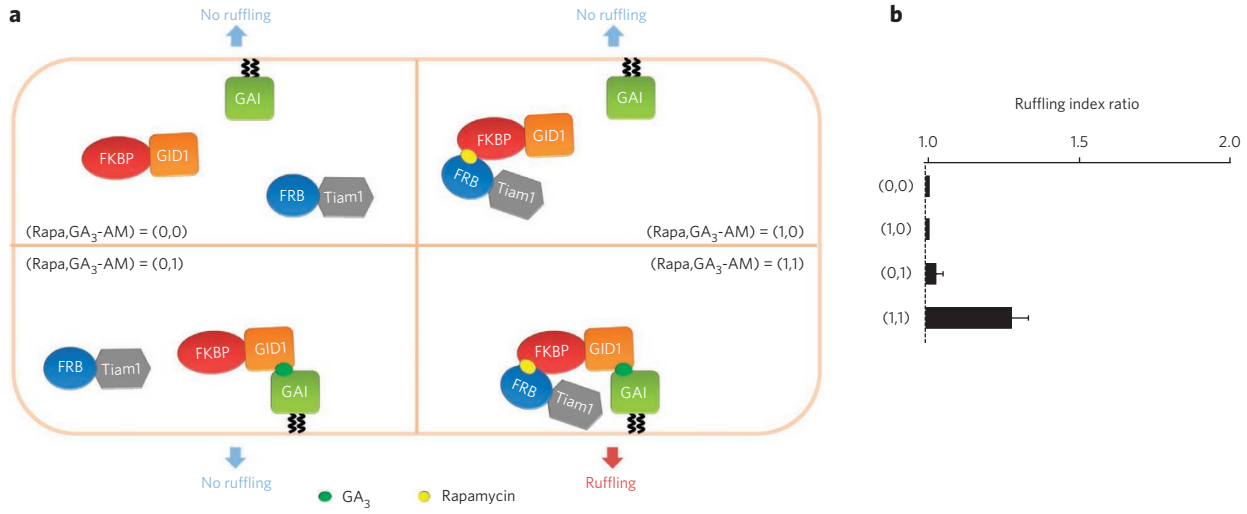

Figure 4 | A fast-processing AND logic gate in living cells using two CID systems. (**a**) Schematic diagram of AND gate using membrane ruffling as output signal. Membrane ruffling was measured for COS-7 cells co-transfected with Lyn-mCherry-GAI$_{1-92}$, FKBP-YFP-GID1 and CFP-FRB-Tiam1 that were subject to treatment with DMSO (representing 0,0 input), rapamycin (Rapa) alone (1,0), GA$_3$-AM alone (0,1) or rapamycin and GA$_3$-AM together (1,1). (**b**) Data from AND gate in **a**. Results are mean and s.e.m. ($n \geq 20$, from three independent experiments).

plasma membrane using a Lyn signal sequence, whereas mCherry-GAI$_{1-92}$ was anchored to the mitochondria using another signal sequence from Tom20 (ref. 27). These four constructs were transfected into COS-7 cells. When GA$_3$-AM and rapamycin were added sequentially, each dimerizer induced protein translocation to its expected intracellular location. Rapamycin did not affect the gibberellin system, or vice versa, verifying their orthogonal nature (**Fig. 2c** and **Supplementary Movie 1**). To induce protein translocation at the same time, we simultaneously added the chemical dimerizers. This induced rapid, coincident translocation of CFP-FKBP and YFP-GID1 to the plasma membrane and mitochondria, respectively (**Supplementary Fig. 11**).

Excessive gibberellin induces acidification in cells

Gibberellin induces acidification in plant cells[37]. To test whether addition of GA$_3$-AM induces acidification in mammalian cells, we monitored pH in cells using a Venus fluorescent protein containing a one-residue substitution (H148G) to make it sensitive to proton concentration in the environment[38]. We co-transfected Venus H148G and CFP to titrate the ratio of Venus fluorescence to CFP at various extracellular pHs with chemical protonophores (that is, monensin and nigericin). At 100 μM, the concentration we generally used for the experiments described above, GA$_3$-AM did not induce detectable acidification in COS-7 cells (**Supplementary Fig. 12**). GA$_3$-AM (100 μM) reduced the pH from 7.4 to 7.3 in HeLa cells. At 100 μM, GA$_3$ did not induce acidification in either cell type, supporting its inefficient membrane permeability. Higher concentration of GA$_3$-AM induced a greater shift in pH, suggesting that the concentration of GA$_3$-AM should be monitored carefully. However, the EC$_{50}$ is much lower than 100 μM, suggesting that efficient dimerization can be induced without any acidification. We used 10 μM GA$_3$-AM for subsequent experiments.

Intracellular logic gates using GA$_3$-AM and rapamycin CID

To construct intracellular CID-based logic gates, we used our newly developed gibberellin-mediated dimerization system that works with a speed comparable to the rapamycin system. First, we created an OR gate whose two inputs are rapamycin and GA$_3$-AM and whose output is an optical signal such as fluorescence. Our design placed two dimerization units at the plasma membrane (Lyn-CFP-FRB-GAI$_{1-92}$) and their binding partner units in the cytoplasm (FKBP-YFP-GID1). We predicted an increase in the FRET signal when FKBP-YFP-GID1 associates with Lyn-CFP-FRB-GAI$_{1-92}$; this should occur in the presence of rapamycin, GA$_3$-AM or both. When these two constructs were transfected in cells, we observed a robust FRET signal with these drug treatments but not with control DMSO treatment (**Supplementary Fig. 13**). The timescale of the process was 60 s.

In addition to speed, versatility is a strength of CID systems. We and others have developed a variety of rapamycin-triggered molecular probes[1], suggesting that chemically inducible logic gates potentially produce various signaling outputs. To pursue this possibility, we used an existing module to produce a second-messenger–mediated output. We used Tiam1-based Rac activation probes in our logic gates and visualized changes in cell morphology as a result of Rac activation. For this OR gate, we transfected cells with the constructs Lyn-CFP-FRB-GAI and FKBP-YFP-Tiam1-GID1 (**Fig. 3a**). We observed membrane ruffling 60–90 s after the addition of chemical dimerizers that induced recruitment of Tiam1 fusion protein to the plasma membrane. Quantitative analysis indicated that the number of cells showing membrane ruffling was significantly greater after the addition of rapamycin, GA$_3$-AM, and both rapamycin and GA$_3$-AM (**Fig. 3b**). It is important to have a clear threshold for an output signal for an accurate computation; this is possible to achieve with our system owing to a very low background output in the absence of either input signal (0,0) that is clearly distinguishable from the output for other single or double-input signals (1,0), (0,1) and (1,1). To demonstrate that other logic gates are possible with the use of orthogonal CID systems, we created an AND gate in which there should be positive output only if both inputs are positive. Our AND gate harbors three components, with GAI$_{1-92}$ at the plasma membrane and FKBP-GID1 and FRB-Tiam1 in the cytoplasm (**Fig. 4a**); we used the specific constructs Lyn-mCherry-GAI$_{1-92}$, FKBP-YFP-GID1 and CFP-FRB-Tiam1. When all three constructs were transfected into COS-7 cells, we observed a significant increase in membrane ruffling only when both GA$_3$-AM and rapamycin were added, but not when either inducer was used alone (**Fig. 4b**).

DISCUSSION

We have developed a new, efficient protein dimerization system using chemically modified gibberellin. With this system, we demonstrated inducible protein recruitment and manipulation of

signaling molecules on a timescale of seconds. Furthermore, the system is completely orthogonal to the existing rapamycin-mediated dimerization system and thus is suited for multivalent manipulation of different molecules at different locations. We then used these two orthogonal chemical dimerization systems to create representative logic gates that process on a timescale of seconds. This is hundreds of times faster than the computation achieved by prevailing logic gates with genetic circuits (tens of minutes to hours) in living cells. In addition to speed, logic gates need to be networked to carry out higher-order computation. The genetic circuits are well suited for this purpose because an output signal from one logic gate can be used as an input signal for another neighboring logic gate, thus readily accommodating several logic gates in a given space[39,40]. In contrast, networking logic gates is challenging for CID systems, as they cannot easily dispense chemical dimerizers as an output signal. Nontrivial engineering would be required to make cells release particular chemical dimerizers. The knowledge obtained through the construction of logic gates using proteins may deepen understanding of 'physiological' logic gates such as coincidence detectors (for example, inositol trisphosphate receptor, adenylate cyclase, AP-2, N-WASP and so on).

An advantage of the use of protein signaling as an output signal is that each protein has a distinctive feature, so an output signal is not limited to a binary code. In this study, we show that FRET and membrane ruffling can serve as an output signal, comprising 4-bit information. We and others have developed many chemically inducible molecular probes that can be used to further expand information size. Other plant hormones dimerize different sets of proteins in plants as gibberellin does[12,30]. With multiple triggers by various plant hormones, input signals could be diversified for more complicated logic gates. Another important aspect of computers is reversibility. The dissociation speed of the two present chemically inducible systems is slow compared with their association speed. Rapid reversibility may allow these logic gates to carry out more useful computation.

METHODS

Chemical synthesis of gibberellin analogs GA_3-AM and GA_3-H. All reagents and solvents were supplied by commercial sources without further purification. All dry solvents were purchased from Aldrich in Sure Seal bottles. Reactions involving air- and/or moisture-sensitive reagents were carried out in an argon atmosphere using glassware dried under vacuum with a heat gun. The evacuated flask was then filled with argon. Reactions were monitored by TLC using Analtech chromatography plates (silica gel GHLF, 250 μm). Visualization was carried out by staining with 10% (w/v) phosphomolybdic acid stain in ethanol. Flash silica gel chromatography was carried out using a Grace Reveleris flash chromatography system equipped with UV and evaporative light-scattering detectors. ^{1}H-NMR (400 MHz) spectra recorded in either deuterated methanol (CD_3OD) or deuterated dimethyl sulfoxide (DMSO-d6) were referenced to a residual solvent peak of 3.31 p.p.m. or 2.50 p.p.m., respectively. ^{13}C NMR (100 MHz) spectra recorded in either CD_3OD or DMSO-d6 were referenced to a residual solvent peak of 49.0 p.p.m. or 39.52 p.p.m., respectively. High-resolution MS mass spectra were recorded at the University of California Riverside Mass Spectrometry Facility. A synthetic scheme of GA_3-AM and GA_3-H is described in more detail in **Supplementary Methods**.

Live-cell confocal and epifluorescence microscopy. The majority of live-cell dual-color or tricolor imaging was done with a spinning-disk confocal microscope. CFP and YFP excitations were conducted with a helium-cadmium laser and argon laser (CVI-Melles Griot), respectively. mCherry excitation was conducted with an argon laser. The two lasers were fiber-coupled (OZ optics) to the spinning-disk confocal unit (CSU10; Yokogawa) mounted with dual CFP-YFP dichroic mirrors (Semrock). The lasers were processed with appropriate filter sets for CFP, YPF and mCherry (Chroma Technology) to capture fluorescence images with a charge-coupled device camera (Orca ER, Hamamatsu Photonics) driven by Metamorph 7.5 imaging software (Molecular Devices). Images were taken using a 40× objective (Zeiss) mounted on an inverted Axiovert 200 microscope (Zeiss). Some additional imaging was done with an epifluorescence microscope. CFP and YFP excitation were carried out by an X-Cite Series 120Q mercury vapor lamp and processed through appropriate filter cubes. Images were taken using a 63× objective (Zeiss) mounted on an inverted Axiovert 135 TV microscope (Zeiss) and were captured by a QIClick charge-coupled device camera (QImaging). Time-lapse live cell imaging was done every ~15 s at ~22–24 °C.

Cytosolic pH measurements in live cells. Intracellular pH change upon addition of 100 (or 333) μM gibberellin derivatives (GA_3 or GA_3-AM) was evaluated using fluorescent protein variant (Venus H148G) and CFP. The H148G mutant is optimal for measuring cytosolic pH because it has a pK_a of ~8. CFP is an internal reference, as it has a pK_a ~4.5. Between 1 d and 2 d after transfection, cells were imaged at ~22–24 °C. Calibration of fluorescence intensity of (Venus H148G and CFP) in living cell was done with 5 μM of each ionophore, nigericin and monensin, in medium over pH range 5–9.

FRET measurement in live cells. Fluorescence images were taken every 15 s as described above. Images were normally collected for 2 min before addition of GA_3, GA_3-AM or rapamycin dissolved in DMSO (0.1% v/v), and then were collected for 8 min after addition of drug. FRET between CFP and YFP was normalized to mean of the reading for the five time points immediately before addition of drug. Graphs represent mean of three independent experiments of 10–15 cells per experiment.

***In vitro* FRET binding assay.** Transient co-transfection of CFP-GAI_{1-92} and YFP-GID1 was carried out using FuGeneHD (Promega) in Cos-7 cells. At 24 h after transfection, cells were lysed in lysis buffer containing 20 mM Tris-HCl, pH 7.5, 120 mM NaCl, 1 mM DTT, 1 mM PMSF, 1 mM EDTA, 5 mM $MgCl_2$, protease inhibitor cocktail (Roche), phosphatase inhibitor cocktail 2 (Sigma-Aldrich) and 1% (v/v) NP-40, and cleared lysates were subjected to *in vitro* FRET assay. Using an EPI fluorescence microscope, fluorescence images were taken 0 and 2 min after addition of either DMSO (control), GA_3 or GA_3-AM. The ratio of CFP-YFP FRET between these two time points was calculated and normalized to the value obtained from DMSO treatment. When eserine (Sigma) was used, it was added to the lysate before the beginning of the assay.

Membrane translocation assay. Fluorescence images were taken every 15 s during the translocation assay. Membrane translocation induced by GA_3-AM dissolved in DMSO (0.1% v/v) was evaluated by fitting the initial part of the normalized time course of the decrease in cytoplasmic fluorescence signal intensity to the exponential function e^{-rt}, where r is the rate constant used as an index of membrane translocation and t is time.

Quantification of ruffling. Membrane ruffles were defined as undulating membrane protrusions, folding back and extending forward, that did not adhere. Membrane ruffles were distinguished from lamellipodia by observation of the dorsal plane. The extent of ruffling of each cell was scored using a scale of 1–3, where 1 indicates that no ruffles were present, 2 indicates that ruffling was confined to isolated regions covering ≤25% of the peripheral area, and 3 indicates that extensive ruffles were present, covering >25% of the peripheral area[41]. Cells with a score of 3 before drug addition were excluded from analysis. We calculated the ratio of the ruffling index (poststimulus/prestimulus) for >20 cells from three independent experiments.

Visualization of esterase activity in living cells. Calcein-AM (ANASPEC) was added to live Cos-7 cells at 100 μM for 30 s; this was immediately followed by washout of extracellular medium before time-series fluorescence imaging on an epifluorescence microscope. Cells were prestained with cholera toxin subunit B labeled with a dye (CTB AlexaFluor 555 from Invitrogen) to ensure the contour of cells.

Statistical analysis. Statistical analysis was done with an unpaired two-tailed Student's *t*-test assuming the two populations have the same variances.

Received 13 July 2011; accepted 2 February 2012; published online 25 March 2012

References

1. Fegan, A., White, B., Carlson, J.C. & Wagner, C.R. Chemically controlled protein assembly: techniques and applications. *Chem. Rev.* **110**, 3315–3336 (2010).
2. Schreiber, S., Kapoor, T.M. & Wess, G. *Chemical Biology: from Small Molecules to Systems Biology and Drug Design*. (Wiley-VCH, 2007).
3. Ho, S.N., Biggar, S.R., Spencer, D.M., Schreiber, S.L. & Crabtree, G.R. Dimeric ligands define a role for transcriptional activation domains in reinitiation. *Nature* **382**, 822–826 (1996).
4. Rivera, V.M. *et al.* A humanized system for pharmacologic control of gene expression. *Nat. Med.* **2**, 1028–1032 (1996).
5. Spencer, D.M., Wandless, T.J., Schreiber, S.L. & Crabtree, G.R. Controlling signal transduction with synthetic ligands. *Science* **262**, 1019–1024 (1993).
6. Komatsu, T. *et al.* Organelle-specific, rapid induction of molecular activities and membrane tethering. *Nat. Methods* **7**, 206–208 (2010).
7. Korzeniowski, M.K., Manjarres, I.M., Varnai, P. & Balla, T. Activation of STIM1-Orai1 involves an intramolecular switching mechanism. *Sci. Signal.* **3**, ra82 (2010).
8. Suh, B.C., Inoue, T., Meyer, T. & Hille, B. Rapid chemically induced changes of PtdIns(4,5)P2 gate KCNQ ion channels. *Science* **314**, 1454–1457 (2006).

9. Ueno, T., Falkenburger, B.H., Pohlmeyer, C. & Inoue, T. Triggering actin comets versus membrane ruffles: distinctive effects of phosphoinositides on actin reorganization. *Sci. Signal.* **4**, ra87 (2011).
10. Bayle, J.H. *et al.* Rapamycin analogs with differential binding specificity permit orthogonal control of protein activity. *Chem. Biol.* **13**, 99–107 (2006).
11. Czlapinski, J.L. *et al.* Conditional glycosylation in eukaryotic cells using a biocompatible chemical inducer of dimerization. *J. Am. Chem. Soc.* **130**, 13186–13187 (2008).
12. Liang, F.S., Ho, W.Q. & Crabtree, G.R. Engineering the ABA plant stress pathway for regulation of induced proximity. *Sci. Signal.* **4**, rs2 (2011).
13. Liberles, S.D., Diver, S.T., Austin, D.J. & Schreiber, S.L. Inducible gene expression and protein translocation using nontoxic ligands identified by a mammalian three-hybrid screen. *Proc. Natl. Acad. Sci. USA* **94**, 7825–7830 (1997).
14. Seelig, G., Soloveichik, D., Zhang, D.Y. & Winfree, E. Enzyme-free nucleic acid logic circuits. *Science* **314**, 1585–1588 (2006).
15. Stojanovic, M.N. Molecular computing with deoxyribozymes. *Prog. Nucleic Acid Res. Mol. Biol.* **82**, 199–217 (2008).
16. Yoshida, W. & Yokobayashi, Y. Photonic Boolean logic gates based on DNA aptamers. *Chem. Commun. (Camb.)* 195–197 (2007).
17. Katz, E. & Privman, V. Enzyme-based logic systems for information processing. *Chem. Soc. Rev.* **39**, 1835–1857 (2010).
18. Qian, L. & Winfree, E. A simple DNA gate motif for synthesizing large-scale circuits. *J. R. Soc. Interface* **8**, 1281–1297 (2011).
19. Rackham, O. & Chin, J.W. Cellular logic with orthogonal ribosomes. *J. Am. Chem. Soc.* **127**, 17584–17585 (2005).
20. Rinaudo, K. *et al.* A universal RNAi-based logic evaluator that operates in mammalian cells. *Nat. Biotechnol.* **25**, 795–801 (2007).
21. Anderson, J.C., Voigt, C.A. & Arkin, A.P. Environmental signal integration by a modular AND gate. *Mol. Syst. Biol.* **3**, 133 (2007).
22. Guet, C.C., Elowitz, M.B., Hsing, W. & Leibler, S. Combinatorial synthesis of genetic networks. *Science* **296**, 1466–1470 (2002).
23. Mayo, A.E., Setty, Y., Shavit, S., Zaslaver, A. & Alon, U. Plasticity of the cis-regulatory input function of a gene. *PLoS Biol.* **4**, e45 (2006).
24. Bronson, J.E., Mazur, W.W. & Cornish, V.W. Transcription factor logic using chemical complementation. *Mol. Biosyst.* **4**, 56–58 (2008).
25. Santner, A. & Estelle, M. Recent advances and emerging trends in plant hormone signalling. *Nature* **459**, 1071–1078 (2009).
26. Ueguchi-Tanaka, M. *et al.* Gibberellin insenstitive DWARF1 encodes a soluble receptor for gibberellin. *Nature* **437**, 693–698 (2005).
27. Hirano, K., Ueguchi-Tanaka, M. & Matsuoka, M. GID1-mediated gibberellin signaling in plants. *Trends Plant Sci.* **13**, 192–199 (2008).
28. Ueguchi-Tanaka, M. *et al.* Molecular interactions of a soluble gibberellin receptor, GID1, with a rice DELLA protein, SLR1, and gibberellin. *Plant Cell* **19**, 2140–2155 (2007).
29. Tsien, R.Y. A non-disruptive technique for loading calcium buffers and indicators into cells. *Nature* **290**, 527–528 (1981).
30. Nishimura, K., Fukagawa, T., Takisawa, H., Kakimoto, T. & Kanemaki, M. An auxin-based degron system for the rapid depletion of proteins in nonplant cells. *Nat. Methods* **6**, 917–922 (2009).
31. Griffiths, J. *et al.* Genetic characterization and functional analysis of the GID1 gibberellin receptors in *Arabidopsis*. *Plant Cell* **18**, 3399–3414 (2006).
32. Hirano, K. *et al.* Characterization of the molecular mechanism underlying gibberellin perception complex formation in rice. *Plant Cell* **22**, 2680–2696 (2010).
33. Inoue, T., Heo, W.D., Grimley, J.S., Wandless, T.J. & Meyer, T. An inducible translocation strategy to rapidly activate and inhibit small GTPase signaling pathways. *Nat. Methods* **2**, 415–418 (2005).
34. Murase, K., Hirano, Y., Sun, T.P. & Hakoshima, T. Gibberellin-induced DELLA recognition by the gibberellin receptor GID1. *Nature* **456**, 459–463 (2008).
35. Shimada, A. *et al.* Structural basis for gibberellin recognition by its receptor GID1. *Nature* **456**, 520–523 (2008).
36. Malgaroli, A., Milani, D., Meldolesi, J. & Pozzan, T. Fura-2 measurement of cytosolic free Ca^{2+} in monolayers and suspensions of various types of animal cells. *J. Cell Biol.* **105**, 2145–2155 (1987).
37. Swanson, S.J. & Jones, R.L. Gibberellic acid induces vacuolar acidification in barley aleurone. *Plant Cell* **8**, 2211–2221 (1996).
38. Tojima, T. *et al.* Attractive axon guidance involves asymmetric membrane transport and exocytosis in the growth cone. *Nat. Neurosci.* **10**, 58–66 (2007).
39. Regot, S. *et al.* Distributed biological computation with multicellular engineered networks. *Nature* **469**, 207–211 (2011).
40. Tamsir, A., Tabor, J.J. & Voigt, C.A. Robust multicellular computing using genetically encoded NOR gates and chemical 'wires'. *Nature* **469**, 212–215 (2011).
41. Ihara, S., Oka, T. & Fukui, Y. Direct binding of SWAP-70 to non-muscle actin is required for membrane ruffling. *J. Cell Sci.* **119**, 500–507 (2006).

Acknowledgments

This study was supported in part by the US National Institutes of Health (NIH; GM092930 and DK090868 to T.I. and NS072241 to M.J.W), the US National Science Foundation (IOS-0641548 and MCB-0923723 to T.S.) and the National Center for Research Resources of the NIH and NIH Roadmap for Medical Research (UL1 RR 025005 to C.M. and D.J.M). T.U. is a recipient of a fellowship from the Japanese Society for the Promotion of Science. M.C. is a recipient of the Provost's Undergraduate Research Award.

Author contributions

T.M., A.S., M.C. and T.I. generated DNA constructs and T.M., R.D., T.U., A.S. and T.I. carried out cell biology experiments. T.S. advised on design of the gibberellin system. T.M. conducted biochemical experiments under supervision of M.J.W. C.M. and D.J.M. synthesized GA_3-AM and GA_3-H. T.I. conceived ideas. R.D. and T.I. wrote the paper.

Competing financial interests

The authors declare competing financial interests: details accompany the full-text HTML version of the paper at http://www.nature.com/naturechemicalbiology/.

Additional information

Supplementary information and chemical compound information is available online at http://www.nature.com/naturechemicalbiology/. Reprints and permissions information is available online at http://www.nature.com/reprints/index.html. Correspondence and requests for materials should be addressed to T.I.